22 Earthquake Early Warning with GPS Data

Simona Colombelli (University of Naples) and Richard Allen

22.1 Introduction

The combined use of seismic and geodetic observations is now a common practice for finite-fault modeling and seismic source parametrization. With the advent of high-rate 1Hz GPS stations the seismological community has recently begun looking at GPS data as a valid complement to the seismic-based methodologies for Earthquake Early Warning (EEW).

In the standard approaches to early warning, the initial portion of the P-wave signal is used to rapidly characterize the earthquake magnitude and to predict the expected ground shaking at a target site, before the arrival of the most damaging waves. Whether the final magnitude of an earthquake can be predicted while the rupture process is underway, still represents a controversial issue; the point is that the limitations of the standard approaches when applied to giant earthquakes have become evident after the experience of the M_w 9.0, 2011 Tohoku-Oki earthquake.

Here we explore the application of GPS data to EEW and investigate whether they can be used to provide reliable and independent magnitude estimations. The large size and the complex rupture process, together with the huge number of high-quality GPS records available, make the 2011 Tohoku-Oki earthquake a unique and ideal case-study for our purposes.

22.2 Seismic vs. GPS data

Because EEW systems are essentially applied to moderate-to-strong earthquakes, large, dynamic, accelerometric sensors are generally used for real-time seismic applications. These instruments are able to record unsaturated signals without risk of clipping at the arrival of the strongest shaking. Accelerometer waveforms are usually integrated twice to obtain displacement time-series and a high-pass causal Butterworth filter is finally applied to remove the artificial effects and long-period drifts introduced by the double integration operation (*Boore*, 2002). The application of the high-pass filter, while removing the artificial distortions, reduces the low-frequency content of the recorded waveforms, resulting in the complete loss of the low-frequency energy radiated by the source and of the static displacement component. The effect of such a filtering is even more relevant for very large earthquakes, whose corner frequency is expected to be lower or comparable with the cut-off filtering frequency (typically 0.075 Hz). Since GPS stations are able to register directly the ground displacement without any risk of saturating and any need of complicated artificial corrections, geodetic displacement time-series represent the complementary contribution to the high-frequency information provided by seismic data.

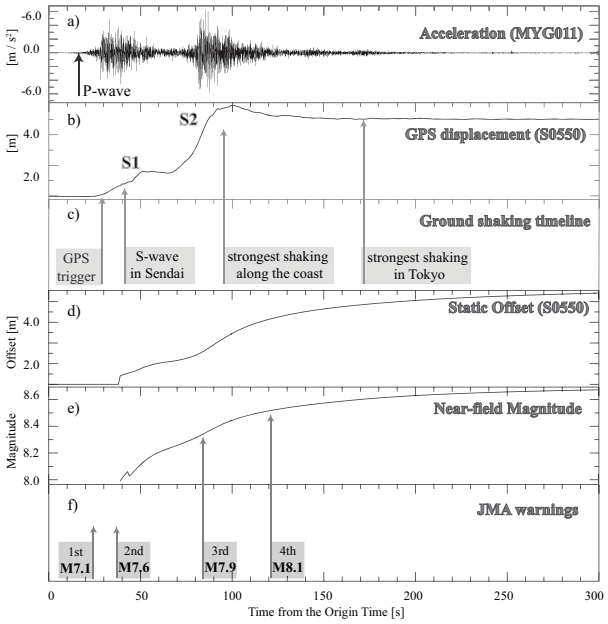

Figure 2.42: a) acceleration waveform at the closest seismic station (MYG011); b) displacement waveform at the closest GPS station (S0550), co-located with MYG011 station; c) timeline showing when the GPS information is available with respect to the time at which the strongest shaking occurs in the Sendai and Tokyo regions; d) output of the algorithm for the static offset extraction at the S0550 station; e) magnitude estimation from the closest GPS station with the point source and the near-field condition approximations; f) timeline of the JMA warnings and magnitude updates.

Figure 2.42 shows a comparison between the acceleration (a) and the GPS displacement (b) waveforms of the Tohoku-Oki earthquake, recorded at two co-located stations (MYG011 from the K-Net network and S0550 from the GEONET network, respectively). Both records show evidence of two main phases (denoted as S1 and S2 in the figure) that correspond to two distinctive, time delayed episodes of slip release during the rupture process (*Lee et al.*, 2011). The GPS displacement starts to be evident later than the P-wave arrival on the seismic record and approximately at the same time of the S-wave arrival and the period of strong shaking. As it can be inferred from the timeline of Figure 2.42c, the P-wave onset at the

closest seismic station (MYG011) occurs approximately 15 seconds after the Origin Time (O.T.), while the first GPS information is available around 40 seconds after the O.T. The maximum amplitude on the GPS record for both phases is almost coherent in time with the arrival of the strongest shaking (on the acceleration waveform) at the same place. However, this does not prevent the use of these data and the issuance of a warning with the expected ground shaking at more distant sites. For example, in the Tokyo region the maximum shaking occurs about 170 seconds after the O.T., well after the GPS displacement has reached its maximum value at the closest station.

22.3 Real-Time offset extraction

We analyzed the co-seismic ground deformations produced by the 2011 Tohoku-Oki earthquake collected by the Japanese GPS Earth Observation Network (GEONET) (*Sagiya*, 2004). In order to extract the permanent displacement, we used the algorithm developed by *Allen and Ziv* (2011). The algorithm looks for a trigger along the records and declares the first-arrival onset when a pre-determined condition on the short-term vs. long-term average is satisfied (*Allen*, 1978). Starting from the trigger time, a running average is then computed along the waveforms and is delivered as a real-time estimation of the static offset. As an example, Figure 2.42d shows the permanent displacement extracted from the S0550 station.

The running average computation is expected to remove the dynamic component of the signal, which would affect the estimation of the static offset. However, to prevent the possible inclusion of a dynamic oscillation, the algorithm starts to deliver the running average after two trigger-amplitude crossings or 10 seconds after the trigger time, whichever comes first.

22.4 Rapid magnitude estimation

The static displacement resulting from the algorithm is then used to obtain a fast estimation of the earthquake magnitude. A quick and preliminary estimation of the earthquake size can be obtained by adopting the theoretical scaling relationship between the earthquake magnitude and the near-field static offset. In case of a very small fault (i.e., a point source) and at short distances from the source (i.e., in the near-field condition), the primary component of the static displacement u can be written as:

$$u \propto \frac{1}{4\pi\mu R^2} M_0(t)$$

where μ is the rigidity modulus of the medium, R the hypocentral distance and $M_0(t)$ the seismic moment. We applied the previous formula to the static offset of the closest station. The result is plotted in Figure 2.42e and shows that the magnitude is fairly well reproduced, despite the approximations and the limited conditions of the formula. This is especially true when our result is compared with the output of the JMA warning system (Figure 2.42f), whose magnitude estimations were largely underestimated for the entire duration of the event. However, a weak systematic underestimation of the final magnitude value (with respect to the official value, $M_w = 9.0$) is evident from the plot. We infer that this underestimation is essentially due to the point source approximation, whose effect may become significant whereas the extended dimension of the fault cannot be neglected.

An approach that may be more robust is inversion for the static slip on the fault plane, which allows consideration of the contributions from the entire fault plane and may provide a better estimation of the earthquake magnitude. We are currently working on the implementation of a real-time static slip inversion scheme using a constant-slip, rectangular source embedded in a homogeneous half-space (*Okada*, 1985). Our goal is to develop an efficient methodology for both the rapid determination of the event size and for the near real-time estimation of the rupture area. This would allow for a correct evaluation of the expected ground shaking at the target sites, that represents, without doubt, the most important aspect of the practical implementation of an early warning system and the most relevant information to be provided to the non-expert, end-user audience.

22.5 Acknowledgements

This work was supported by the University of Naples Federico II and a grant from the Moore Foundation.

22.6 References

Allen, R.V. Automatic earthquake recognition and timing from single traces, *Bull. Seism. Soc. Am., 68,* 5, 1521-1532, 1978.

Allen, R.M. and A. Ziv. Application of real-time GPS to earthquake early warning, *Geophys. Res. Lett., 38,* 2011.

Boore, D.M. Comments on Baseline Correction of Digital Strong-Motion Data: Examples from the 1999 Hector Mine, California, Earthquake, *Bull. Seism. Soc. Am., 92,* 4, 1543-1560, 2002.

Lee, S.-J., B.-S. Huang, M. Ando, H.-C. Chiu, and J.-H. Wang. Evidence of large scale repeating slip during the 2011 Tohoku-Oki earthquake, *Geophys. Res. Lett., 38,* 2011.

Okada, Y. Surface deformation due to shear and tensile faults in a half-space, *Bull. Seism. Soc. Am., 75,* 4, 1135-1154, 1985.

Sagiya, T. A decade of GEONET: 19942003 The continuous GPS observation in Japan and its impact on earthquake studies, *Earth Planets Space, 56,* xxixxli, 2004.